

## *In situ* viscoelastic properties of insoluble and porous polysaccharide biopolymer dextran produced by *Leuconostoc mesenteroides* using particle-tracking microrheology

Min-Kyung Jeon<sup>1a</sup>, Tae-Hyuk Kwon<sup>\*1</sup>, Jin-Sung Park<sup>2b</sup> and Jennifer H. Shin<sup>2c</sup>

<sup>1</sup> Department of Civil and environmental engineering, Korea Advanced Institute of Science and Technology, 291 Daehak-ro, Yuseong-gu, Daejeon 34141, Republic of Korea

<sup>2</sup> Department of Mechanical engineering, Korea Advanced Institute of Science and Technology, 291 Daehak-ro, Yuseong-gu, Daejeon 34141, Republic of Korea

(Received October 18, 2016, Revised December 20, 2016, Accepted February 15, 2017)

**Abstract.** With growing interests in using bacterial biopolymers in geotechnical practices, identifying mechanical properties of soft gel-like biopolymers is important in predicting their efficacy in soil modification and treatment. As one of the promising candidates, dextran was found to be produced by *Leuconostoc mesenteroides*. The model bacteria utilize sucrose as working material and synthesize both soluble and insoluble dextran which forms a complex and inhomogeneous polymer network. However, the traditional rheometer has a limitation to capture *in situ* properties of inherently porous and inhomogeneous biopolymers. Therefore, we used the particle tracking microrheology to characterize the material properties of the dextran polymer. TEM images revealed a range of pore size mostly less than 20  $\mu\text{m}$ , showing large pores  $> 2 \mu\text{m}$  and small pores within the solid matrix whose sizes are less than 1  $\mu\text{m}$ . Microrheology data showed two distinct regimes in the bacterial dextran, purely viscous pore region of soluble dextran and viscoelastic region of the solid part of insoluble dextran matrix. Diffusive beads represented the soluble dextran dissolved in an aqueous phase, of which viscosity was three times higher than the growth medium viscosity. The local properties of the insoluble dextran were extracted from the results of the minimally moving beads embedded in the dextran matrix or trapped in small pores. At high frequency ( $\omega > 0.2 \text{ Hz}$ ), the insoluble dextran showed the elastic behavior with the storage modulus of  $\sim 0.1 \text{ Pa}$ . As frequency decreased, the insoluble dextran matrix exhibited the viscoelastic behavior with the decreasing storage modulus in the range of  $\sim 0.1\text{--}10^3 \text{ Pa}$  and the increasing loss modulus in the range of  $\sim 10^4\text{--}1 \text{ Pa}$ . The obtained results provide a compilation of frequency-dependent rheological or viscoelastic properties of soft gel-like porous biopolymers at the particular conditions where soil bacteria produce bacterial biopolymers in subsurface.

**Keywords:** complex shear modulus; biopolymer; dextran; particle tracking micro-rheology

### 1. Introduction

In geotechnical engineering, there are various movements to use microbial by-products for improving the soil properties including bioclogging, bio-cementation, and bio-remediation (Chang

---

\*Corresponding author, Assistant Professor, E-mail: [t.kwon@kaist.ac.kr](mailto:t.kwon@kaist.ac.kr)

<sup>a</sup> Graduate Student, E-mail: [gmk909@kaist.ac.kr](mailto:gmk909@kaist.ac.kr)

<sup>b</sup> Research Professor, E-mail: [jinsugp9@kaist.ac.kr](mailto:jinsugp9@kaist.ac.kr)

<sup>c</sup> Professor, E-mail: [j\\_shin@kaist.ac.kr](mailto:j_shin@kaist.ac.kr)

and Cho 2012, Chang *et al.* 2015, 2016, Mitchell and Santamarina 2005, Sidik *et al.* 2014). Use of formation of bacterial biopolymers or biofilms has garnered significant interest as a promising means to cause bioclogging, reducing permeability, increasing strength, and eventually to seal cracks or leakage in geotechnical earth structures (Chang and Cho 2014, Mitchell and Santamarina 2005, Pintelon *et al.* 2012, Yasodian *et al.* 2012). Indigenous microbial communities in subsurface ubiquitously exhibit their ability to produce insoluble *soft* polysaccharidic biopolymers either as their habitats or as byproducts of their metabolisms. Owing to such ubiquity and versatility, it has been studied for feasibility of using bacterial biopolymers for soil modification and leakage sealing (Abdel Aal *et al.* 2010, Blauw *et al.* 2009, Cunningham *et al.* 1991, 2003, Noh *et al.* 2016, Taylor and Jaffé 1990). For evaluation of the efficacy of these treatments in practices, the engineering properties of biopolymer itself, such as mechanical and hydraulic properties, are required as the part of the effective mixture models to predict the behavior of biopolymer-formed soils. However, viscoelastic behaviors of soft biopolymers produced by bacterial activities remains poorly identified. Moreover, this class of bacterial biopolymers shows the inherent porous and inhomogeneous natures as produced in an aqueous environment; this is blocking the reliable measurement of the mechanical properties of soft matters.

Herein, we present the viscoelastic properties of insoluble and porous biopolymers produced by bacteria. In this study, insoluble polysaccharidic biopolymers, referred to as dextran, were prepared by culturing and stimulating *Leuconostoc mesenteroides*. Because traditional rheometers requires a considerable amount of the target material and measures its bulk properties, assuming homogeneous distribution across the sample, it is not suitable for the inherently porous and inhomogeneous biopolymers studied herein. Therefore, the particle-tracking microrheology (PTM) which only requires small amounts of a sample (Mason *et al.* 1997) was used, thereby, the local and microscale viscoelastic behaviors of the microbially produced biopolymers were investigated while overcoming the inherent inhomogeneous and porous nature. In particular, the frequency-dependent complex shear moduli of *in situ* insoluble dextran for the intact solid part and liquid-filled void part were successfully obtained and compared with previously reported data. The obtained microscale properties are expected to be implemented for modeling of soil particle-soft biopolymer interactions at the particle scale.

## 2. Theoretical background

### 2.1 Rheology

Rheology is the study of flow and deformation of viscoelastic materials. The viscoelastic or rheological properties of viscoelastic materials can be expressed with the frequency-dependent complex modulus ( $G^*$ ), as follows

$$G^*(\omega) = G'(\omega) + i \cdot G''(\omega) \quad (1)$$

where  $\omega$  is the frequency (Hz), the real part of the complex modulus ( $G^*$ ) is referred to as the storage modulus ( $G'$ ) and the imaginary part is called as the loss modulus ( $G''$ ). The storage modulus indicates the in-phase modulus and represents the elastic energy storage, so thus the elasticity of materials. On the other hand, the loss modulus indicates the out-of-phase modulus and represents the viscous energy loss. For instance, for a perfectly elastic material,  $G'$  is constant and  $G''$  is zero. In contrast, for a viscous liquid,  $G'$  is zero and  $G''$  is equal to  $\eta \cdot \omega$ , where  $\eta$  is the

viscosity of fluid (Pa·s) (Wirtz 2009).

### 2.2 Particle-tracking microrheology (PTM)

Particle-tracking microrheology (PTM) uses the Brownian motions of small particles, which are excited by thermal energy. The trajectory of these particles can be converted to the diffusion coefficient of surrounding materials using the Stokes relation, as follows (Dasgupta and Weitz 2005, Mason and Weitz 1995, Wirtz 2009)

$$D = \frac{k_B T}{\xi}, \tag{2}$$

where  $D$  is the diffusion coefficient ( $\text{m}^2 \cdot \text{s}^{-1}$ ),  $k_B$  is the Boltzmann constant ( $\text{m}^2 \cdot \text{kg} \cdot \text{s}^{-2} \cdot \text{K}^{-1}$ ),  $\xi$  is the friction factor of particle ( $\text{kg} \cdot \text{s}^{-1}$ ), and  $T$  is the absolute temperature (K). Particles should be small enough to ignore inertia effect, generally smaller than  $1 \mu\text{m}$  in diameter, so as to exhibit the Brownian motions with the diffusion coefficient  $D$ . By the Stokes relation, the friction factor of particle  $\xi$  is defined as follows

$$\xi(i\omega) = 6\pi\eta(i\omega)a, \tag{3}$$

where  $\eta$  is the Laplace frequency  $i\omega$  is the Laplace frequency-dependent viscosity, and  $a$  is the particle radius. Einstein relation (fluctuation-dissipation theorem) means that mean square displacement (MSD) have relations

$$\langle \Delta x(\tau)^2 \rangle = 2D\tau, \tag{4}$$

where  $\langle \Delta x(\tau)^2 \rangle$  is the mean square displacement (MSD) in  $x$ -direction during the lag time  $\tau$ . When the experiment is conducted in two dimensions and it is assumed that the material is isotropic, MSD is expressed as follows (Wirtz 2009)

$$\begin{aligned} \langle \Delta r(\tau)^2 \rangle &= \langle (r(t+\tau) - r(t))^2 \rangle \\ &= \langle (x(t+\tau) - x(t))^2 \rangle + \langle (y(t+\tau) - y(t))^2 \rangle = 4D\tau \end{aligned}, \tag{5}$$

where  $\langle \Delta r(\tau)^2 \rangle$  is the MSD in  $x$ - and  $y$ -direction during the lag time  $\tau$  (Crocker *et al.* 2000). By combining Eqs. (2)-(5), the Stokes-Einstein relation can be expressed as follows

$$\tilde{G}(i\omega) = \frac{k_B T}{\pi a \cdot (i\omega) \cdot \langle (\Delta \tilde{r}(i\omega))^2 \rangle}. \tag{6}$$

Thereafter,  $\tilde{G}(i\omega)$  is transformed algebraically to Fourier frequency dependent shear modulus  $G^*(\omega)$  by using power law (Dasgupta *et al.* 2002). Finally, the storage modulus and the loss modulus can be calculated by using the following formulations

$$G(\omega) = \frac{k_B T}{\pi a \langle (\Delta r(1/\omega))^2 \rangle \Gamma(1 + \alpha(\omega)) [1 + \frac{\beta(\omega)}{2}]}, \tag{7}$$

$$G'(\omega) = G(\omega) \frac{1}{1 + \beta'(\omega)} \cos \left[ \frac{\pi}{2} \alpha'(\omega) - \beta'(\omega) \alpha'(\omega) \left( \frac{\pi}{2} - 1 \right) \right], \text{ and} \quad (8)$$

$$G''(\omega) = G(\omega) \frac{1}{1 + \beta'(\omega)} \sin \left[ \frac{\pi}{2} \alpha'(\omega) - \beta'(\omega) [1 - \alpha'(\omega)] \left( \frac{\pi}{2} - 1 \right) \right], \quad (9)$$

where  $\Gamma$  denotes the gamma function,  $\alpha(\omega)$  is the first-order logarithmic time derivatives of MSD,  $\beta(\omega)$  is the second-order logarithmic time derivatives of MSD,  $\alpha'(\omega)$  is the local first-order logarithmic derivatives of  $G(\omega)$ , and  $\beta'(\omega)$  is the local second-order logarithmic derivatives of  $G(\omega)$ . Note that  $\omega$  is the frequency (Hz), and  $\tau$  is the lag time (s), equal to  $1/\omega$ .

### 3. Materials and method

#### 3.1 Model bacteria and biopolymers

*Leuconostoc mesenteroides* NRRL-B523 (ATCC 14935) was chosen as the model. These model bacteria are gram-positive and facultative anaerobes, such that they grow well in both aerobic and anaerobic conditions (Zurera-Cosano *et al.* 2006). In the presence of sucrose, the bacteria are known to produce insoluble biopolymer, dextran, by synthesizing sucrose and fructose by using dextransucrase that is also produced by *L. mesenteroides* (Padmanabhan and Kim 2002).

Dextran is a polysaccharide made of glucose molecules and mainly composed of  $\alpha$ -1,6 glycosidic bonds with partial  $\alpha$ -1,3 linkages. The structural heterogeneity of dextran is affected by the presence of non- $\alpha$ -1,6 linkages, and it is reported that the frequency and extent of such heterogeneity increases with the percentage of non- $\alpha$ -1,6 linked units in the branched polysaccharide dextran (Wilham *et al.* 1955). There are three classes of dextran (i.e., class 1, class 2, and class 3), and the dextran produced by *L. mesenteroides* NRRL-B523 are classified as class 3 that shows porous and heterogeneous nature due to the high percentage of consecutive  $\alpha$ -1,3 linkages (Naessens *et al.* 2005, Wilham *et al.* 1955). In this study, *L. mesenteroides* were aerobically cultured in the defined growth medium, following Lappan and Fogler (1994) and Noh *et al.* (2016) (Table 1). After two days cultivation, it was confirmed that the model bacteria produced insoluble dextran.

#### 3.2 Sample preparation

##### 3.2.1 Sample preparation for particle-tracking microrheology

Fig. 1 illustrates the procedure for dextran sample preparation. The inoculum of the model bacteria was prepared by mixing the culture grown in the growth medium at 30°C for two days

Table 1 Growth medium composition

Component	Concentration
Sucrose	40 g/L
Yeast extract	10 g/L
1M phosphate monobasic	41 ml/L
1M phosphate dibasic	59 ml/L

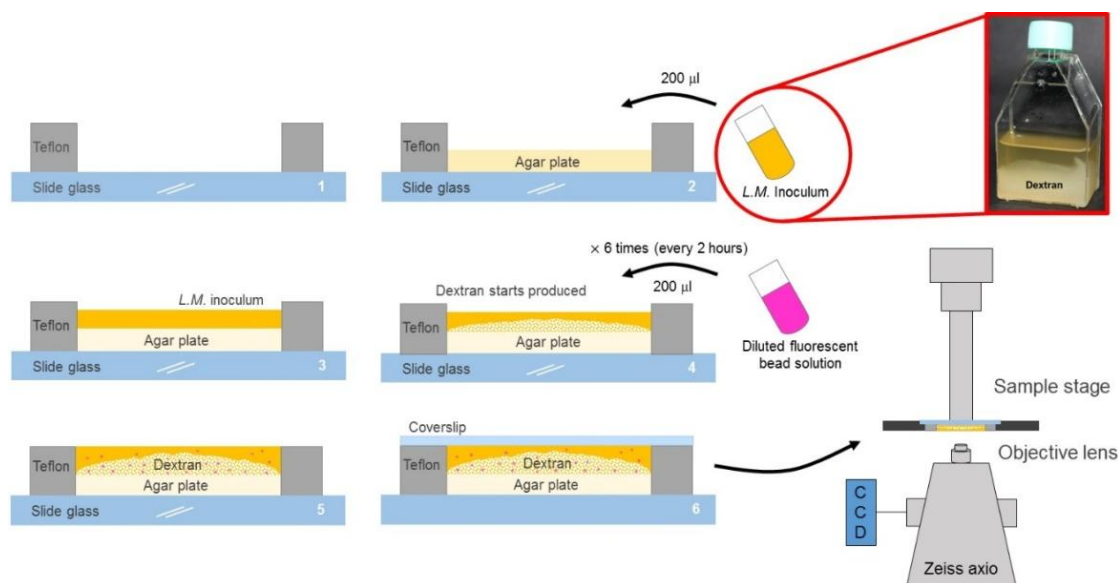


Fig. 1 Experiment setup and sample preparation

and the fresh medium with the volume ratio of 1:10 (or 1:10 v/v). To measure the rheological properties at *in situ* condition, an agar plate was prepared on a slide glass, as shown in Fig. 1. The agar medium was prepared by mixing agar (Difco Bacto agar) with the growth medium at 2% w/w concentration. A droplet of 200  $\mu\text{L}$  inoculum in an exponential growth phase was placed on the agar plate. The fluorescent bead solution (0.5  $\mu\text{m}$  diameter; F8812, Thermo Fisher) was diluted with the growth medium (1:10000 v/v). After 12 hours, when small amounts of dextran were produced, the diluted fluorescent bead solution of 200  $\mu\text{L}$  was spread every two hours on the produced dextran surface for 12 hours. The addition of the beads was carefully carried out to evenly distribute and smear them in the dextran structure. Additional 12 hours later, the agar plate, which was full of dextran and the liquid growth medium, were sealed with a coverslip and vacuum grease for PTM, as illustrated in Fig. 1.

### 3.2.2 Sample preparation for transmission electron microscopy (TEM) imaging

Sample preparation for the transmission electron microscopy (TEM) imaging followed the procedure for the microrheology sample preparation, up to the part of the dextran production on an agar plate. Herein, the diluted fluorescent bead solution was not added. Thereafter, the produced insoluble dextran was separated from the slide glass, and the bacteria were fixed by formaldehyde and dehydrated with alcohol. Then, the dextran sample was solidified by using epoxy resin. Finally, the solidified dextran sample was cut to have 100 nm thickness using microtome (Ultracuts UTC).

### 3.3 Imaging and data reduction for particle-tracking microrheology

Two-dimensional trajectories of fluorescent beads were captured by the inverted fluorescent microscope (Zeiss Axio Lab.A1) instrumented with the high-speed CCD (Zyla sCMOS 5.5; Andor), the 63x objective lens, and the rhodamine fluorescent light. To capture the movements of the beads in the dextran part, the prepared sample was placed upside down, as shown in Fig. 1. All imaging experiments were conducted at 25°C. Two frame rates were used: 100 frames per seconds

for high frequency cases (or H cases) and one frame per second for low frequency cases (L cases). One thousand images were captured; in other words, the durations of image recording were 10 s for H cases and 1000 s for L cases.

From the time-lapsed recorded images, the time-varying coordinates of each bead were calculated over the duration to obtain the trajectory of beads. Herein, we assumed that the center of the bead showed the maximum brightness. Following the procedure suggested by Crocker *et al.* (2007), the  $x$  and  $y$  coordinates of the bead centers were estimated and their trajectories with time were obtained.

## 4. Results and discussion

### 4.1 Pore size distribution

The presence of internal pores in our dextran produced by *L. mesenteroides* strain was confirmed in the images obtained from the environmental scanning electron microscopy (ESEM), as shown in Fig. 2(a). By analyzing this image, the pore size distribution was obtained, in which the effective pore radius was calculated from the area of each pore, as shown in Fig. 2(b). The radius of pores in dextran ranged from 1 to 100  $\mu\text{m}$  and  $\sim 95\%$  of the radius was less than 20  $\mu\text{m}$ . Although it was difficult to determine the size of small nanoscale pores less than 1  $\mu\text{m}$  (or nano-pores) because of the limited resolution of ESEM, the small nanoscale pores can be presumed with high likelihood to exist in the dextran structure. Therefore, it can be expected that the fluorescent beads in large pores at microscale (or micro-pores) would be more affected by the viscous liquid surrounding the beads rather than the intact solid dextran. Therefore, we can anticipate that the beads in micro-pores exhibit a diffusive behavior while the beads in nano-pores show a partially or completely bounded viscoelastic behavior. This was also confirmed by TEM images. Some fluorescent beads were positioned in the large micro-pores (see Fig. 2(c)), while the other beads were trapped in the intact solid dextran matrix (see Fig. 2(d)).

### 4.2 Mean square displacement (MSD) results

The trajectories of the fluorescent beads were obtained via the image analysis. Fig. 3 shows the traced trajectories of the beads in the dextran sample for 10 s (H case). It was found that the beads exhibited the two extreme motions: diffusive movements (Fig. 3(a)) and minimal movements (Fig. 3(b)). Accordingly, all results were classified into two classes: the diffusive behavior as class A and the minimal movement as class B.

Using Eq. (5), the obtained trajectories were converted into the mean square displacement (MSD) values with respect to the lag time. Fig. 4 shows the variations in the MSD values  $\langle \Delta r(\tau)^2 \rangle$  with the lag time  $\tau$ , i.e., MSD traces. Ambient oscillating noises in the MSD traces were removed by applying the moving-average with a window size of 10.

Assuming that the MSD values are proportional to  $\tau^\alpha$ , the exponent  $\alpha$  represents the slope of the MSD trace in the log-log scale (Fig. 4). For class A, the exponent  $\alpha$  was  $\sim 0.88$  for the lag time interval of 0.1–3 s (H case; Fig. 4(a)). In other words, the class A exhibits the rheological behavior of viscous liquid as the MSD of pure viscous liquid shows the exponent  $\alpha$  close to one. The trajectories of class A beads for low frequency (L case) were not captured because the beads were too diffusive, such that the beads disappeared out of the field of view. For class B, the exponent  $\alpha$  was estimated to range 0.015–0.016 for the lag time interval of 0.1–5 s (H case) and 0.14 and 0.88

for the 5–30 s and 40–80 s intervals (L case), respectively. It was noted that the MSD values of class B were time-independent for that short duration of 0.1–5 s (H case), which implies that dextran showed elastic characteristic at a high frequency range (~0.2–10 Hz). Whereas, in L case, the sub-diffusive  $\alpha$  exponent ( $0 < \alpha < 1$ ) indicates the dextran showed a viscoelastic behavior for the long duration of 5–30 s or for a low frequency range (~0.03–0.2 Hz). We obtained the MSD traces of the known materials for reference, de-ionized water (DI water) as viscous liquid and polydimethylsiloxane (PDMS) as an elastic material. As shown in Fig. 4(a), the MSD trace of class A dextran shows approximately two times higher value than that of DI water, but with the same slope with respect to the lag time. Given the high stiffness of PDMS, the MSD trace of PDMS was perfectly flat, but its values were ~10 times less than those of class B dextran. This comparison confirms the diffusive behavior of class A dextran and the elastic or viscoelastic behavior of class B dextran at these high frequencies (0.2–10 Hz).

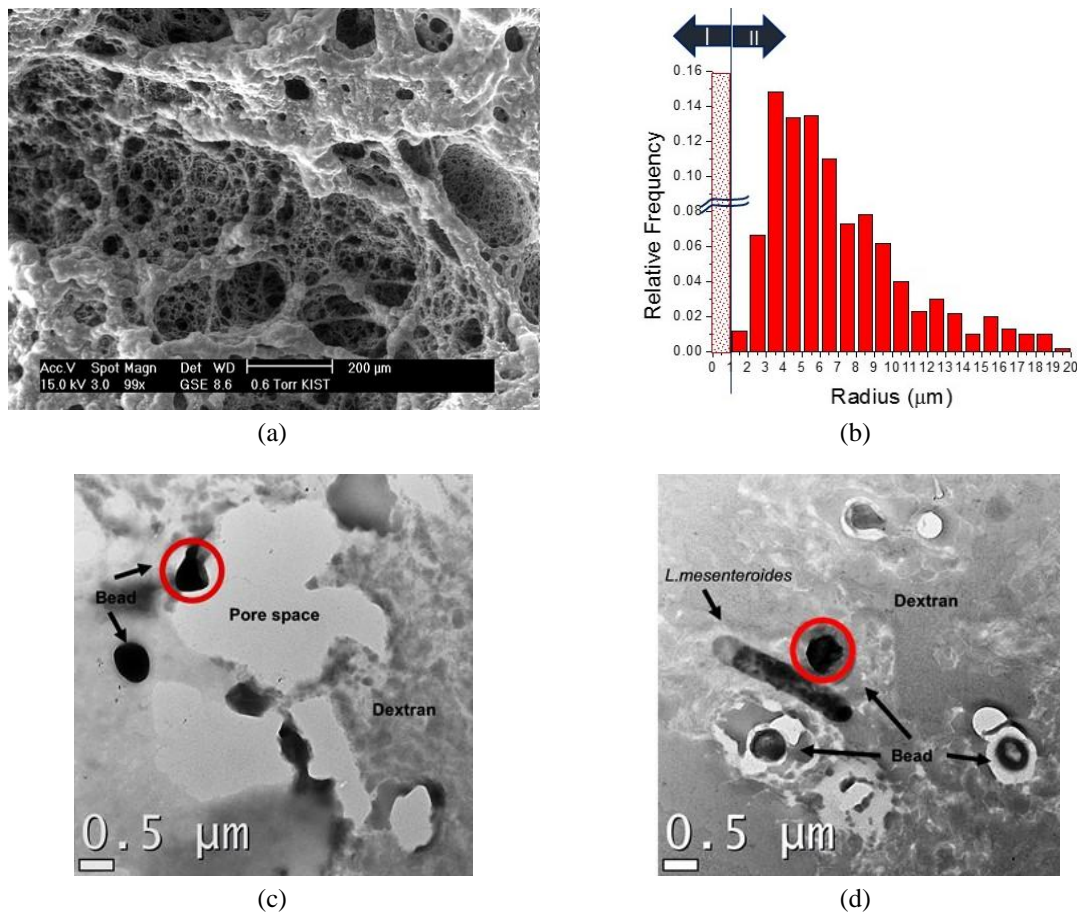


Fig. 2 (a) An ESEM image of porous dextran; and (b) the pore size distribution obtained from the ESEM image; (c) A TEM image of the beads that are partially embedded in the large pores; and (d) a TEM image of the beads embedded in intact solid dextran matrix or in small pores smaller than the fluorescent bead radius. Some empty spaces around beads in Fig. 2(d) were produced during the process of TEM sample preparation, especially microtome, because the thickness of TEM samples were 100 nm

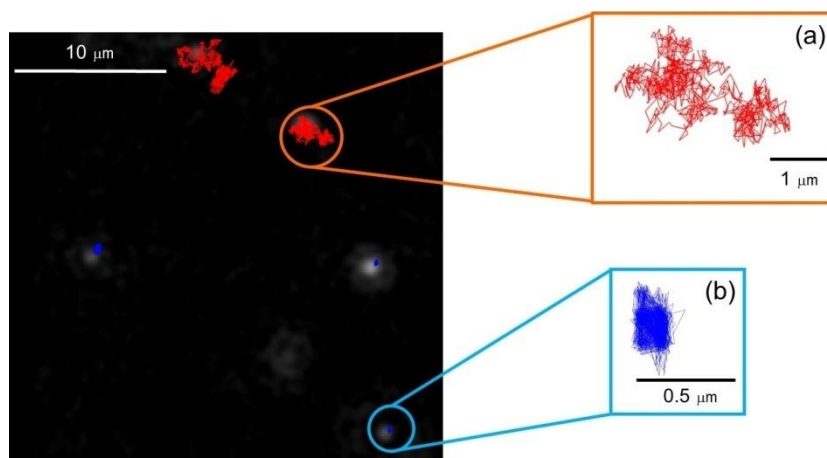


Fig. 3 The captured trajectories of the fluorescent beads: (a) diffusive bead (class A); (b) minimal movement bead (class B)

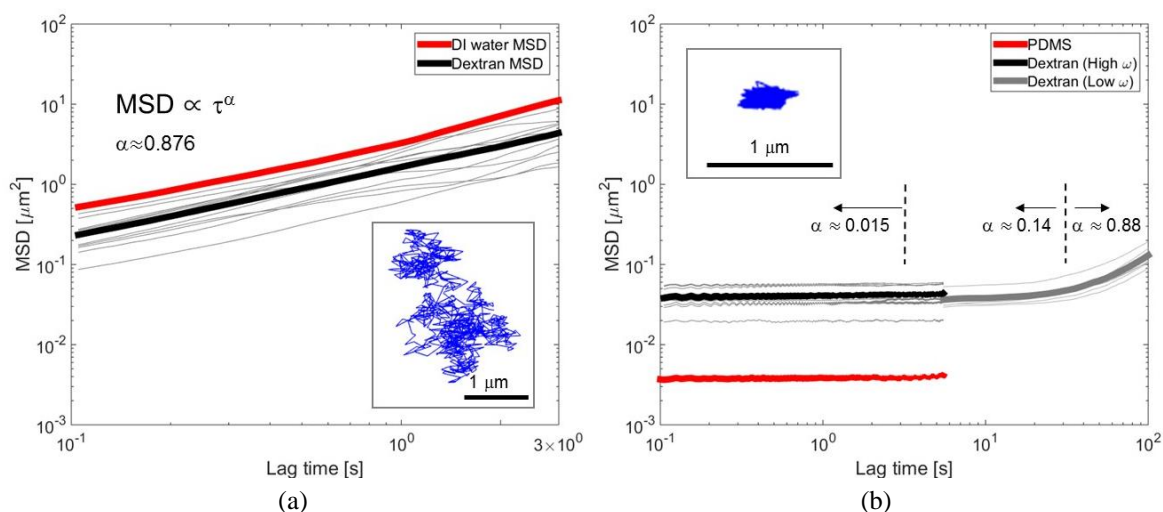


Fig. 4 Mean square displacement (MSD) of beads in dextran against the lag time: (a) diffusive beads (class A) and (b) beads with minimal motions (class B). The red lines indicate the reference results, which are viscous liquid and elastic solid ((a) DI water; and (b) PDMS), respectively

#### 4.3 Frequency-dependent complex shear moduli and viscosity

The frequency-dependent complex shear moduli for classes A and B were calculated from the MSD traces by using Eqs. (7)-(9), as shown in Figs. 5 and 6. In addition, the complex viscosity  $\eta^*(\omega)$  was computed using the following relation

$$\eta^*(\omega) = \sqrt{G'(\omega)^2 + G''(\omega)^2} / \omega \quad (10)$$

For class A, the loss modulus  $G''$  was larger than the storage modulus  $G'$ , as can be expected

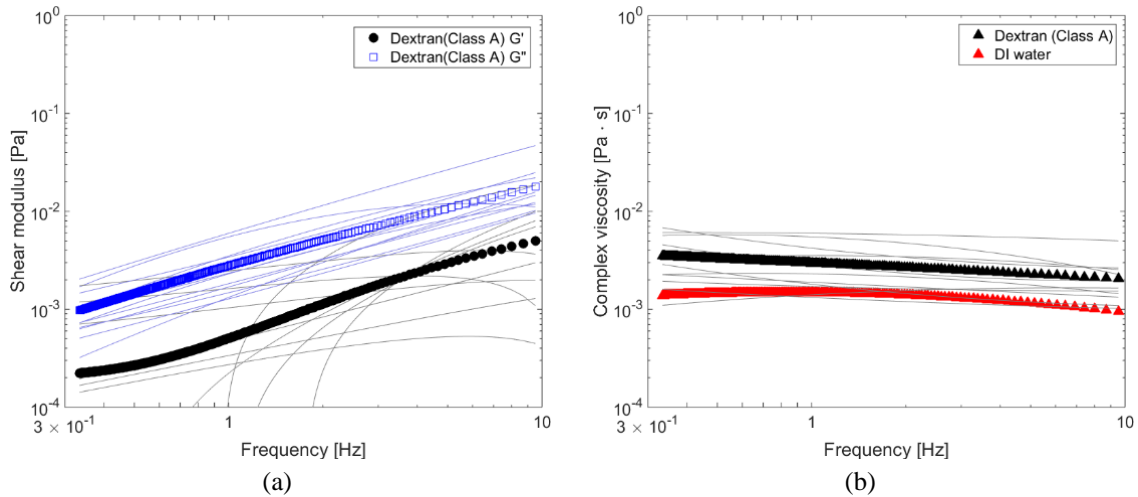


Fig. 5 Frequency-dependent complex shear modulus and viscosity of class A: (a) storage and loss moduli and (b) complex viscosity. The red line indicates the viscosity of DI water obtained by PTM

from the MSD results (Fig. 5(a)). The loss modulus and the storage modulus at 1 Hz were  $\sim 3 \cdot 10^{-3}$  Pa and  $\sim 5 \cdot 10^{-4}$  Pa, respectively. The viscosity at 1 Hz was  $\sim 3 \cdot 10^{-3}$  Pa · s. Given that the viscosity of 4% (w/w) sugar solution, which is equivalent to our growth medium, is 1.11 times greater than that of DI water (i.e.,  $\sim 1.11 \cdot 10^{-3}$  Pa · s), the viscosity range of class A was approximately three times greater than the viscosity of the growth medium (Fig. 5(b)) (Swindells 1958). Thus, it was found that the bead motions for class A were affected not by the solid dextran but by the liquid growth medium. This observation on the high loss modulus and high viscosity for class A is presumably attributed to the soluble dextran produced by the model bacteria *L. mesenteroides* B523. It is

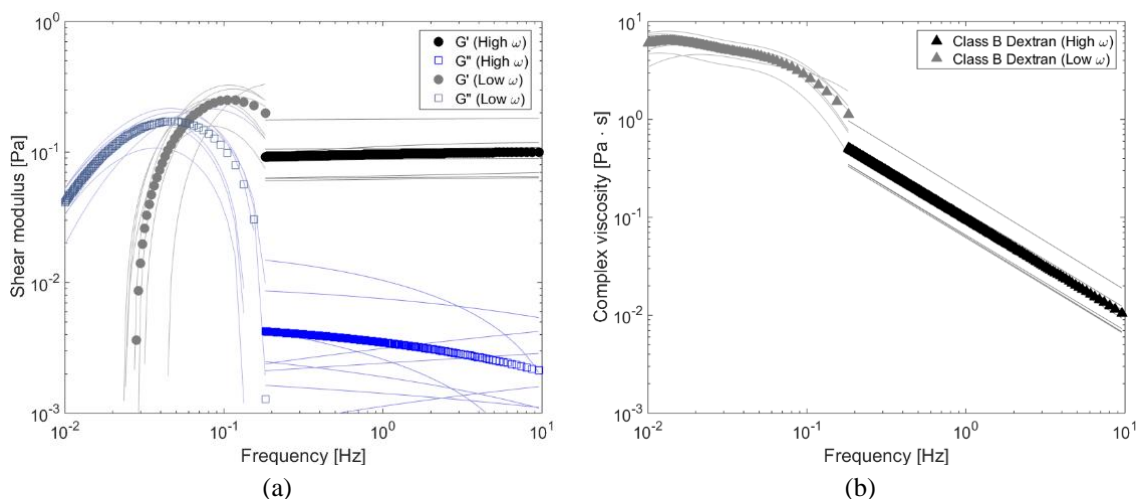


Fig. 6 Frequency-dependent complex shear modulus and viscosity of class B: (a) storage and loss moduli: and (b) complex viscosity. Discontinuity in Fig. 6(a) and 6(b) resulted from the truncation error in converting the MSD results to the shear moduli

because *L. mesenteroides* B523 produced not only the insoluble dextran but also the soluble dextran, and this soluble dextran is being widely used for viscosity controlling agents (Naessens *et al.* 2005).

The MSD traces of class B confirmed that the beads were properly trapped in the insoluble dextran, thereby the complex moduli and viscosity of class B represent the local rheological properties of the *intact solid part* of insoluble dextran *in situ* conditions, as shown in Fig. 6. In the high frequency  $\omega > 0.2$  Hz, the storage modulus  $G'$  was consistently not affected by frequency; it was much larger than the loss modulus  $G''$  by more than one order of magnitude. This indicates the high elasticity of dextran at such high frequency. The storage modulus and the loss modulus were  $\sim 0.1$  Pa and  $\sim 0.003$  Pa at 1 Hz (Fig. 6(a)). On the contrary, for the low frequency for  $\omega < 0.2$  Hz, the loss modulus was comparable to or even larger than the storage modulus, implying highly viscoelastic behavior. Accordingly, it was observed that the complex viscosity ranged  $\sim 1$ – $10$  Pa·s for  $\omega = 0.01$ – $0.2$  Hz and it decreased with an increase in frequency, which is a typical behavior of non-Newtonian fluids, referred to as the shear-thinning effect (Fig. 6(b)) (Mezger 2006).

Over the tested frequency range, the results indicate that the insoluble dextran shows the highly elastic behavior in a high frequency range ( $\omega > 0.2$  Hz) while it exhibited the viscoelastic behavior with some viscosity in a low frequency range ( $\omega < 0.2$  Hz).

#### 4.4 Discussion – Comparison with other biopolymers

The results of class A reflect the rheological properties (complex moduli and viscosity) of viscous liquid containing soluble dextran, which fills large micro-pores in the solid dextran matrix. The complex moduli ranged 0.0002–0.004 Pa for the storage modulus and 0.001–0.02 Pa for the loss modulus for  $\omega = 0.3$ – $10$  Hz. The viscosity was  $\sim 0.002$ – $0.003$  Pa·s because of the soluble dextran produced by *L. mesenteroides*. Whereas, the results of class B represent the viscoelastic properties of the intact solid part or the solid matrix of insoluble dextran itself, where the complex moduli ranged 0.05–0.2 Pa for the storage modulus and 0.001–0.01 Pa for the loss modulus for  $\omega = 0.01$ – $10$  Hz. The viscosity decreased from  $\sim 10$  to 0.01 Pa·s for  $\omega = 0.01$ – $10$  Hz.

Table 2 compares the rheological properties of various bacterial biopolymers and biofilms gathered from previous studies though only limited experiment results are available. For the frequency  $\omega = 1$  Hz, the gel solution (high acyl gellan gel and xanthan gum in Table 2) generally had the stiffness values of in the order of 1–100 Pa, which are 2–3 orders of magnitude larger than that of insoluble dextran (Choppe *et al.* 2010, Flores-Huicochea *et al.* 2013). *Streptococcus mutans* produce biofilms, which consist of polysaccharides and small amounts of proteins (Cheong *et al.* 2009). These polysaccharides have the similar structure to that of insoluble dextran. Their experiment conditions in Cheong *et al.* (2009) were also similar to ours though the sample preparation method was different. In their study, the concentration of polysaccharide was controlled by dissolving in water and NaOH solution after precipitation by cold ethanol. In our study, the dextran concentration in a liquid phase was not controllable because bacteria were directly stimulated *in situ* to produce dextran for a given growth condition. Despite the difference in the polysaccharide concentrations, the complex moduli of the soluble polysaccharide from *S. mutans* (Choppe *et al.* 2010) were close to our results of class A. Contrary to that, the complex moduli of the insoluble polysaccharide from *S. mutans* (Cheong *et al.* 2009) were 100–1000 times larger than our results of class B. This large difference is attributed to the difference in concentration owing to their sample preparation procedure, where a significantly large amount of insoluble polysaccharide was separated from *S. mutans* cultures (Cheong *et al.* 2009). Furthermore,

Table 2 Rheological values of biomaterials in previous study

Material	Condition	Method	Storage modulus at 1 Hz	Loss modulus at 1 Hz	Reference
High acyl gellan (HAG) gel	0.5% gel, 30°C	Rheometer (ARES RFS III)	~90–100 Pa	~2–3 Pa	Flores-Huicochea <i>et al.</i> (2013)
Xanthan gum	10 g/L, 50°C	Rheometer	~5–10 Pa	~10–20 Pa	Choppe <i>et al.</i> (2010)
Soluble polysaccharide from <i>S. mutans</i>	20% gel, room temperature	Holographic microrheology	~5·10 <sup>-4</sup> –10 <sup>-3</sup> Pa	~0.008–0.01 Pa	Cheong <i>et al.</i> (2009)
Insoluble polysaccharide from <i>S. mutans</i>	20% gel, room temperature	Holographic microrheology	~10–20 Pa	~7–10 Pa	Cheong <i>et al.</i> (2009)
Insoluble dextran from <i>L. mesenteroides</i> B523	Freeze dried, 250 mg/ml, room temperature	Rheometer	~10 <sup>4</sup> Pa	~10 <sup>4</sup> –2·10 <sup>4</sup> Pa	Padmanabhan <i>et al.</i> (2003)
Biofilm of <i>S. aureus</i>	In situ, 37°C, 7 hours incubation	Passive microrheology	~0.1–0.2 Pa (at 100 Hz)	~0.07–0.08 Pa (at 100 Hz)	Rogers <i>et al.</i> (2008)
Dextran from <i>L. mesenteroides</i> B523	In situ, 30°C 1 days incubation	Passive microrheology	~5·10 <sup>-4</sup> Pa for soluble dextran (Class A) ~0.1 Pa for insoluble dextran (Class B)	~3·10 <sup>-3</sup> Pa	This study

the rheometer test results on dextran (Padmanabhan *et al.* 2003) also showed the larger complex moduli than class B results. On the top of concentration difference, this is in part attributed to the scale difference because microrheology measures the local properties of inhomogeneous materials while the conventional rheometer, such as the one used in Padmanabhan *et al.* (2003) captures the bulk properties.

Meanwhile, in Rogers *et al.* (2008), the rheological parameters of biofilms were measured by *in situ* PTM, which is consistent with ours. The storage modulus was ~0.1–0.2 Pa and the loss modulus was ~0.07–0.08 Pa at 100 Hz. While the frequency difference may still cause difficulty in direct comparison, the ranges of the storage and loss moduli were similar between *Staphylococcus aureus* biofilm and the insoluble dextran from *L. mesenteroides*. Thus, it can be concluded that the shear modulus of the solid matrix part of soft polysaccharidic biopolymers or biofilms is ~0.1 Pa for the frequency  $\omega = 0.2$ –10 Hz while the loss modulus is smaller than the storage modulus by one or two order of magnitude, as corroborated by this study and Rogers *et al.* (2008).

## 5. Conclusions

This study investigated the microrheological properties of porous insoluble dextran *in situ*, which was produced by *L. mesenteroides* by using the particle-tracking microrheology (PTM). The main findings are as follows:

- The dextran produced by *L. mesenteroides* strain had the internal pores, and ~95% of the pores was less than 20  $\mu\text{m}$  in radius. Owing to this inherent porous structure of dextran, the MSD traces were classified into two classes: the diffusive beads that were placed in large micro-pores (class A) and the completely embedded beads in the solid matrix part of dextran (class B).
- The diffusive beads appeared to represent the liquid growth medium containing the soluble dextran produced by *L. mesenteroides*. The storage modulus and loss modulus increased from  $2 \cdot 10^{-4}$  to  $2 \cdot 10^{-3}$  Pa and from  $10^{-3}$  to  $2 \cdot 10^{-2}$  Pa, respectively as the frequency increased from 0.3 to 10 Hz. The viscosity of this dextran-dissolved liquid ranged  $\sim 2\text{--}3 \cdot 10^{-3}$  Pa·s, approximately 2–3 times greater than the viscosity of the growth medium.
- The embedded beads captured the viscoelastic behavior of the solid dextran matrix produced by *L. mesenteroides*. In particular, at the high frequency  $\omega > 0.2$  Hz, the dextran exhibited elastic characteristics, with the constant storage modulus values of  $\sim 0.1$  Pa and the negligible loss modulus. For the low frequency for  $\omega < 0.2$  Hz, the solid dextran matrix showed viscous loss, with the loss modulus comparable to the storage modulus and the viscosity of  $\sim 1\text{--}10$  Pa·s.
- After comparing with the previous results, the rheological properties of the insoluble soft polysaccharidic biopolymers produced by bacteria including dextran were found to be in the same order of magnitude with *in situ* bacterial biofilms, with the storage modulus of  $\sim 0.1$  Pa. Meanwhile, the complex shear moduli of extracted or purified biopolymers, gels, and extracellular polymeric substances at highly concentrated forms were 2–3 orders of magnitudes larger than those as they were produced by bacteria *in situ*.

The obtained microscale rheology properties of the intact part of solid dextran and the dextran-dissolved liquid provide information on the viscoelastic behaviors of bacterially produced soft biopolymers, and these are expected to be directly implemented for modeling of soil particle-soft biopolymer interactions.

## Acknowledgments

We are grateful for valuable comments by the reviewers and editors. We would like to thank Je-Hyun Han who helped us in data analysis. This research was supported by the Korea Institute of Energy Technology Evaluation and Planning (KETEP) and the Ministry of Trade, Industry and Energy (MOTIE) of the Republic of Korea (20152520100760), and by Korea Minister of Ministry of Land, Infrastructure and Transport (MOLIT) as U-City Master and Doctor Course Grant Program.

## References

Abdel Aal, G.Z., Atekwana, E.A. and Atekwana, E.A. (2010), "Effect of bioclogging in porous media on

- complex conductivity signatures”, *J. Geophys. Res.: Biogeosci.*, **115**(G3),G00G07.
- Blauw, M., Labert, J.W.M. and Latil, M.N. (2009), “Biosealing: A method for in situ sealing of leakages”, *Proceeding of the International Symposium on Ground Improvement Technologies and Case Histories, ISGI09*, Singapore, December, Volume 9, pp. 125-130.
- Chang, I. and Cho, G.-C. (2012), “Strengthening of Korean residual soil with  $\beta$ -1,3/1,6-glucan biopolymer”, *Constr. Build. Mater.*, **30**, 30-35.
- Chang, I. and Cho, G.-C. (2014), “Geotechnical behavior of a  $\beta$ -1,3/1,6-glucan biopolymer-treated residual soil”, *Geomech. Eng., Int. J.*, **7**(6), 633-647.
- Chang, I., Jeon, M. and Cho, G.C. (2015), “Application of microbial biopolymers as an alternative construction binder for earth buildings in underdeveloped countries”, *Int. J. Polym. Sci.*, **9**.
- Chang, I., Im, J. and Cho, G.-C. (2016), “Introduction of microbial biopolymers in soil treatment for future environmentally-friendly and sustainable geotechnical engineering”, *Sustainability*, **8**(3), 251.
- Cheong, F.C., Duarte, S., Lee, S.H. and Grier, D.G. (2009), “Holographic microrheology of polysaccharides from *Streptococcus mutans* biofilms”, *Rheologica Acta*, **48**(1), 109-115.
- Choppe, E., Puaud, F., Nicolai, T. and Benyahia, L. (2010), “Rheology of xanthan solutions as a function of temperature, concentration and ionic strength”, *Carbohydr. Polym.*, **82**(4), 1228-1235.
- Crocker, J.C. and Hoffman, B.D. (2007), “Multiple-particle tracking and two-point microrheology in cells”, *Methods Cell Biol.*, **83**, 141-178.
- Crocker, J.C., Valentine, M.T., Weeks, E.R., Gisler, T., Kaplan, P.D., Yodh, A.G. and Weitz, D.A. (2000), “Two-point microrheology of inhomogeneous soft materials”, *Phys. Rev. Lett.*, **85**(4), 888.
- Cunningham, A.B., Characklis, W.G., Abedeen, F. and Crawford, D. (1991), “Influence of biofilm accumulation on porous media hydrodynamics”, *Environ. Sci. Technol.*, **25**(7), 1305-1311.
- Cunningham, A.B., Sharp, R.R., Hiebert, R. and James, G. (2003), “Subsurface biofilm barriers for the containment and remediation of contaminated groundwater”, *Bioremed. J.*, **7**(3-4), 151-164.
- Dasgupta, B.R. and Weitz, D. (2005), “Microrheology of cross-linked polyacrylamide networks”, *Phys. Rev. E*, **71**(2), 021504.
- Dasgupta, B.R., Tee, S.-Y., Crocker, J.C., Frisken, B. and Weitz, D. (2002), “Microrheology of polyethylene oxide using diffusing wave spectroscopy and single scattering”, *Phys. Rev. E*, **65**(5), 051505.
- Flores-Huicochea, E., Rodríguez-Hernández, A.I., Espinosa-Solares, T. and Tecante, A. (2013), “Sol-gel transition temperatures of high acyl gellan with monovalent and divalent cations from rheological measurements”, *Food Hydrocolloids*, **31**(2), 299-305.
- Lappan, R.E. and Fogler, H.S. (1994), “*Leuconostoc mesenteroides* growth kinetics with application to bacterial profile modification”, *Biotechnol. Bioeng.*, **43**(9), 865-873.
- Mason, T.G. and Weitz, D. (1995), “Optical measurements of frequency-dependent linear viscoelastic moduli of complex fluids”, *Phys. Rev. Lett.*, **74**(7), 1250.
- Mason, T.G., Ganesan, K., Van Zanten, J.H., Wirtz, D. and Kuo, S.C. (1997), “Particle tracking microrheology of complex fluids”, *Phys. Rev. Lett.*, **79**(17), 3282.
- Mezger, T.G. (2006), *The Rheology Handbook: For Users of Rotational and Oscillatory Rheometers*, Vincentz Network GmbH & Co KG.
- Mitchell, J.K. and Santamarina, J.C. (2005), “Biological considerations in geotechnical engineering”, *J. Geotech. Geoenviron. Eng.*, **131**(10), 1222-1233.
- Naessens, M., Cerdobbel, A., Soetaert, W. and Vandamme, E.J. (2005), “*Leuconostoc dextranase* and dextran: production, properties and applications”, *J. Chem. Technol. Biotechnol.*, **80**(8), 845-860.
- Noh, D.H., Ajo-Franklin, J.B., Kwon, T.H. and Muhunthan, B. (2016), “P and S wave responses of bacterial biopolymer formation in unconsolidated porous media”, *J. Geophys. Res.: Biogeosci.*, **121**(4), 1158-1177.
- Padmanabhan, P.A. and Kim, D.-S. (2002), “Production of insoluble dextran using cell-bound dextranase of *Leuconostoc mesenteroides* NRRL B-523”, *Carbohydr. Res.*, **337**(17), 1529-1533.
- Padmanabhan, P.A., Kim, D.S., Pak, D. and Sim, S.J. (2003), “Rheology and gelation of water-insoluble dextran from *Leuconostoc mesenteroides* NRRL B-523”, *Carbohydr. Polym.*, **53**(4), 459-468.
- Pintelon, T.R., Picioreanu, C., van Loosdrecht, M. and Johns, M.L. (2012), “The effect of biofilm

- permeability on bio-clogging of porous media”, *Biotechnol. Bioeng.*, **109**(4), 1031-1042.
- Rogers, S., Van Der Walle, C. and Waigh, T. (2008), “Microrheology of bacterial biofilms in vitro: Staphylococcus aureus and Pseudomonas aeruginosa”, *Langmuir*, **24**(23), 13549-13555.
- Sidik, W.S., Canakci, H., Kilic, I.H. and Celik, F. (2014), “Applicability of biocementation for organic soil and its effect on permeability”, *Geomech. Eng., Int. J.*, **7**(6), 649-663.
- Stewart, T.L. and Fogler, H.S. (2001), “Biomass plug development and propagation in porous media”, *Biotechnol. Bioeng.*, **72**(3), 353-363.
- Swindells, J.F. (1958), “Viscosities of sucrose solutions at various temperatures: Tables of recalculated values”, Vol. 440; For sale by the Supt. of Docs., USGPO.
- Taylor, S.W. and Jaffé, P.R. (1990), “Biofilm growth and the related changes in the physical properties of a porous medium: 1. Experimental Investigation”, *Water Resour. Res.*, **28**(5), 1481-1482.
- Wilham, C.A., Alexander, B.H. and Jeanes, A. (1955), “Heterogeneity in dextran preparations”, *Arch. Biochem. Biophys.*, **59**(1), 61-75.
- Wirtz, D. (2009), “Particle-tracking microrheology of living cells: Principles and applications”, *Annu. Rev. Biophys.*, **38**, 301-326.
- Yasodian, S.E., Dutta, R.K., Mathew, L., Anima, T.M. and Seena, S.B. (2012), “Effect of microorganism on engineering properties of cohesive soils”, *Geomech. Eng., Int. J.*, **4**(2), 135-150.
- Zurera-Cosano, G., García-Gimeno, R., Rodríguez-Pérez, R. and Hervás-Martínez, C. (2006), “Performance of response surface model for prediction of *Leuconostoc mesenteroides* growth parameters under different experimental conditions”, *Food Control*, **17**(6), 429-438.